



Removal of tetracycline from aqueous solution by hydrothermal method derived titanate nanotubes

Huiyuan Li, Guangxia Li, Jie Wu, Xin Zhong, Hui Zhang*

Department of Environmental Engineering, Wuhan University, P.O. Box C319 Luoyu Road 129[#], Wuhan 430079, China, Tel. +86 27 68775837; emails: 405055098@qq.com (H. Li), liguangxiamanman@gmail.com (G. Li), jei23@126.com (J. Wu), 41964167@qq.com (X. Zhong), Tel. +86 27 68775837; Fax: +86 27 68778893; email: eeng@whu.edu.cn (H. Zhang)

Received 3 December 2014; Accepted 28 September 2015

ABSTRACT

In the present study, the removal of tetracycline (TC) from aqueous solution by titanate nanotubes (TNTs) was investigated. TNTs were synthesized by hydrothermal treatment of the commercial TiO₂ particles. The morphology and structures of the as-prepared products were investigated by transmission electron microscopy, N₂ adsorption/desorption, Fourier transform infrared, and X-ray diffraction. Batch experiments showed that the removal of TC by TNTs was very fast in the first 60 min, and then reached equilibrium after 180 min. The removal efficiency of TC increased with the increase in the dosage of TNTs and the decrease of initial TC concentration. Initial pH also affected the removal process and the optimum initial pH was 5. The kinetic data were better described by the pseudo-second-order model than by the pseudo-first-order model. The equilibrium adsorption data were analyzed with three isotherm models (Langmuir model, Freundlich model, and Temkin model). The data were best fitted with the Langmuir isotherm model with correlation coefficient of 0.9947, corresponding to a maximum adsorption capacity of 113.6 mg/g.

Keywords: Adsorption; Antibiotics; Isotherm; Kinetics; Titanate nanotube

1. Introduction

Pharmaceuticals and personal care products (PPCPs) constitute a group of emerging pollutants in the environment and have drawn growing attention around the world [1–5]. Among them, antibiotics are widely used as human infectious disease medicines, veterinary medicines, and animal husbandry growth promoters [6]. Their widespread use has become a serious problem since their potential adverse effects, including acute and chronic toxicity, impact on aquatic photosynthetic organisms, and disruption of

indigenous microbial populations [7]. They may also cause long-term and irreversible change to the microorganisms genome, increasing the resistance of bacteria against drugs, even at low concentrations [8]. Tetracycline (TC) is a well-known class of antibiotics with a large global consumption in animal food industry to treat, control, and prevent infectious disease. It is also used as a food additive to improve the growth rate of animals at lower cost. The large usage of TC makes them widely spread in the environment [9,10]. Therefore, various technologies have been employed to the removal of TC from aqueous solution [11–13].

Adsorption has been considered to be one of the most promising technologies for removing antibiotics

*Corresponding author.

due to its simplicity in operation and cost-effectivity [14]. In recent years, the removal of TC by various sorbents has been investigated [7,12,15–20]. Among different sorbents, titanate nanotubes (TNTs) are of special interest due to their high specific surface areas and pore volumes as well as good ion exchange properties [21]. TNTs can be synthesized by template-based and electrochemical methods, but they often involve expensive and complex procedures and the minimum size of the nanotubes is commonly limited by the template mold dimension [22]. Alternatively, Kasuga et al. [23] reported the preparation of TNTs as small as 10 nm by a simple hydrothermal treatment of TiO₂ powder in 10 M NaOH aqueous solution and subsequently washed with HCl aqueous solution. This method provided shorter time for synthesis with high yield and reusable alkali solutions [14,21]. In recent years, TNTs have been proved to be efficient for the adsorption of dyes [24–27], heavy metals [21,28,29], and even radionuclides [30,31]. However, to the best of our knowledge, the studies about the removal of TC by TNTs adsorption are still scarce.

In the present work, TNTs were prepared by a hydrothermal reaction and was characterized by transmission electron microscopy (TEM), X-ray diffraction (XRD), and Fourier transform infrared (FTIR). The removal of TC by TNTs adsorption was systematically investigated. The effects of various operational conditions such as initial pH, sorbent dosage, and initial TC concentration were studied. Furthermore, the adsorption kinetics and isotherms were also analyzed.

2. Materials and methods

2.1. Chemicals

The commercial TC (AR Grade, 99%) and TiO₂ particles (Aldrich, ≥99% purity, 325 mesh) were used without further purification. Other chemicals such as sodium hydroxide and hydrochloric acid were of analytical grade. All solutions used in the experiment were prepared with deionized water. The structure and relevant data for TC are shown in Fig. 1. It has different acid groups in its chemical structure and can exist under different ionic species and conformations depending on the solution pH [19].

2.2. TNTs preparation

TNTs were synthesized by a hydrothermal process similar to that reported in the previous study [32]. Typically, 2 g of TiO₂ particles was added to 70 mL of 10 M NaOH aqueous solution in a Teflon-lined stainless steel vessel. After vigorous stirring for 1 h at room

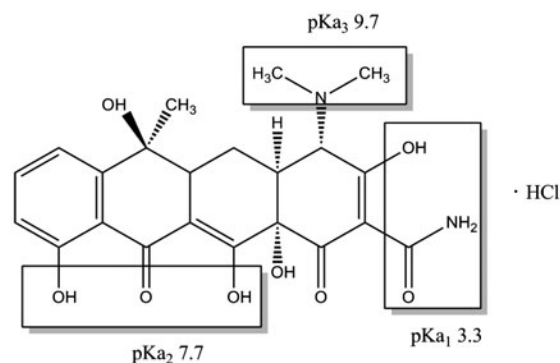


Fig. 1. Chemical structure of TC.

temperature, the mixture had a heat treatment in oven for 24 h at 150°C. Next, the precipitation was stirred in 0.1 M HCl solution for 1 h and washed again with distilled water, then was stirred in 0.1 M HCl for 24 h. After that, the washing procedure using distilled water was repeated until the pH value of the rinsing solution approached the pH value of distilled water. The washed white precipitate obtained was dried in the oven at 80–100°C and TNTs were obtained.

The morphologies of the TNTs were characterized using the TEM analysis, which was conducted with JEM-100CXII microscope operating at 200 kV. Powder XRD patterns were collected on a Bruker AXS D5005 X-ray diffractometer, using a Cu-K α radiation ($\lambda = 1.54184 \text{ \AA}$) as X-ray source. Specific surface area was measured through N₂ adsorption/desorption using a Gemini V2.00 surface area analyzer. For the FTIR investigation, a Nicolet 5700 FTIR spectrometer was used.

2.3. Experimental procedure

All experiments were carried out at room temperature to investigate the removal of TC by TNTs. In a typical experiment, a given amount of TNTs was added to 200 mL of TC aqueous solution. The initial pH (pH₀) of the solution was adjusted by 0.1 M HCl and 0.1 M NaOH. A magnetic stirrer was used to ensure its homogenization for 24 h. At appropriate time intervals, the aliquots were withdrawn from the solution and filtrated immediately with a 0.45- μm membrane to measure the concentration of TC by a Shimadzu UV-9100 spectrophotometer (Shimadzu, Japan) at a wavelength of 275 nm. High-performance liquid chromatography (HPLC), which was consisted of a LC-20AB pump, a Shimadzu HPLC system manager program and a SPD-20A UV-vis detector, was also applied to measure the concentration of TC. The amount of TC adsorbed onto unit weight of adsorbent (q_t) was calculated as follows:

$$q_t = \frac{V \times (C_0 - C)}{m} \quad (1)$$

where V (L) is the solution volume, C_0 (mg/L) is the initial TC concentration, C (mg/L) is the TC concentration at any time t , and m (g) is the dry weight of TNTs.

3. Results and discussion

3.1. Characterization of TNTs

Surface area and porosity are important physical properties that influence the quality and utility of many materials and products. According to N_2 adsorption/desorption experiment, the measured BET

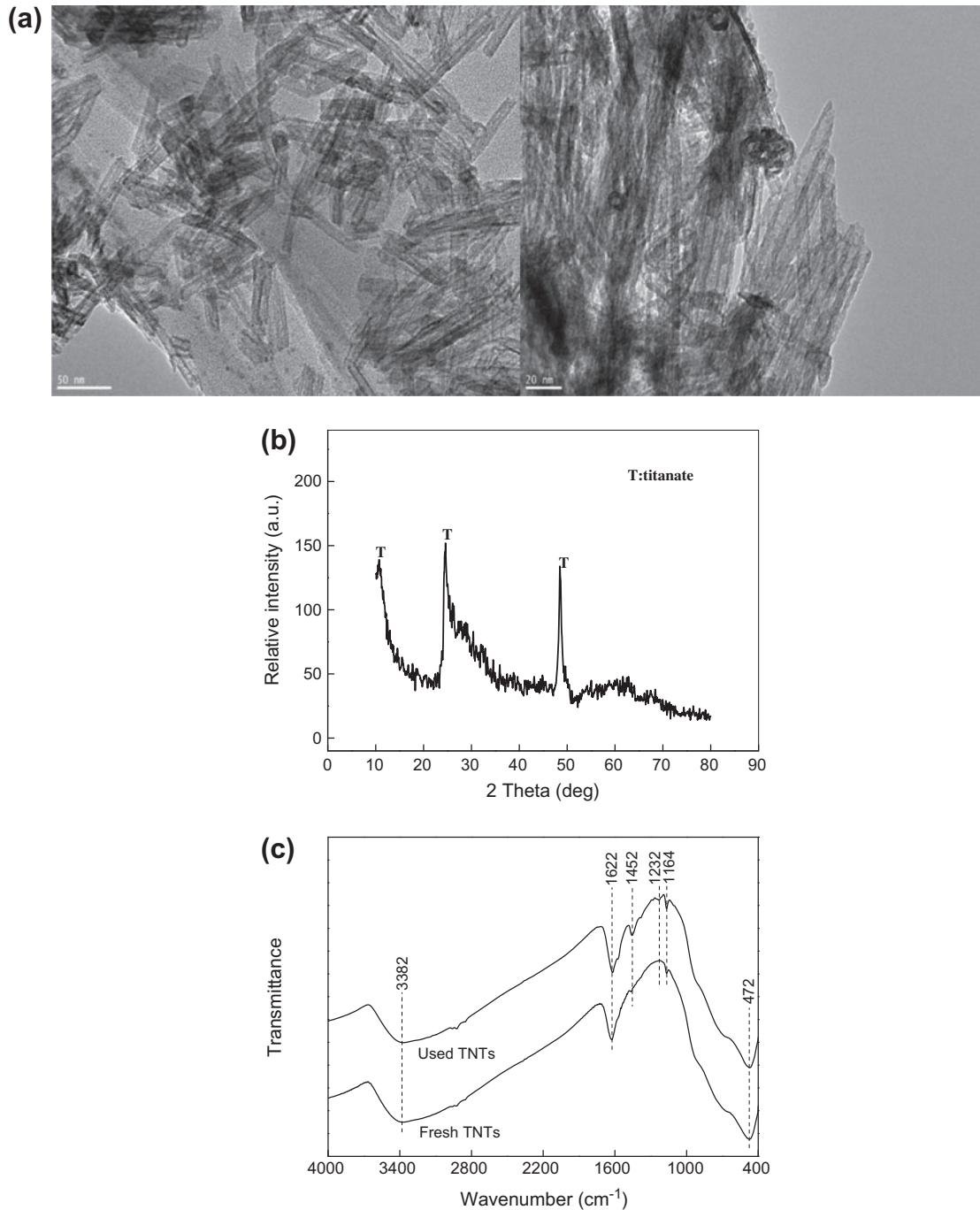


Fig. 2. Characterization of TNTs: (a) TEM images, (b) XRD patterns, and (c) FTIR spectra.

specific surface area and the single-point total pore volume were $155.78 \text{ m}^2/\text{g}$ and $0.38 \text{ cm}^3/\text{g}$, respectively. The value of the surface area was similar with some previous reports [27]. In addition, the average pore diameter was found to be as small as 9.85 nm, indicating that the as-prepared TNTs had small pores.

Fig. 2(a) shows the TEM images of the as-prepared products. It can be seen that a large amount of randomly tangled nanotubes was obtained. These tubes were shown to be hollow and open-ended. Also, unequal number of walls scrolling on the two tube sides was observed from the TEM micrograph. The TEM images indicated that the outer diameter of the TNTs was in the range of 6–10 nm, whereas the inner diameter of the tubes were measured to be about 4–6 nm, which was in good consistency with the previous studies [27]. The lengths were measured to be approximately 100 nm.

Fig. 2(b) presents the XRD patterns of the TNTs. No anatase or rutile phases were detected in the XRD spectra of TNTs. The intense peak at about 10° was ascribed to interlayer space of TNTs, in accordance with the previous reports [22,25–27,30]. Two characteristic peaks positioned at $2\theta \approx 26^\circ, 48^\circ$ in the diffraction of TNTs, were assigned to diffraction of hydrogen titanate compounds according to the standard XRD data [25]. As reported in the literature [33], all the peaks can be indexed based on an $\text{H}_2\text{Ti}_3\text{O}_7$ structure (monoclinic unit cell with $a = 1.603$, $b = 0.375$, $c = 0.919$ nm, and $\beta = 101.45^\circ$). $\text{H}_2\text{Ti}_3\text{O}_7$ behaves as a weak Bronsted acid, however, it is usually described as titanium hydroxide oxide [$\text{Ti}_3(\text{OH})_2\text{O}_5$] and can be stable in alkali solutions. The original titanium particles were probably first transformed to sodium titanates through hydrothermal treatment, and then the sodium titanate products changed to hydrogen titanate after washing in acidic solution through an ion exchange mechanism [25].

Fig. 2(c) presents the FTIR spectra of the fresh and used TNTs. The spectra indicated the presence of a large amount of water and hydroxyl groups in the TNTs because of the existence of a bending vibration of H–O–H at $1,622 \text{ cm}^{-1}$ and a strong stretching vibration of O–H at $3,382 \text{ cm}^{-1}$ [24]. The broad band (from about 800 till 400 cm^{-1}) was assigned to Ti–O and Ti–O–Ti skeletal frequency region [34]. As for the used TNTs, a new band at around $1,452 \text{ cm}^{-1}$ appeared, which was attributed to the in-plane skeletal vibrations of aromatic ring. The results indicated that TC adsorption took place on the TNTs surface, and their interaction yielded the new band.

3.2. Effect of initial pH on TC removal

The removal of TC by Aldrich TiO_2 particles and TNTs were firstly conducted to investigate the

adsorption performance of TNTs. It can be seen in Fig. 3 that the removal efficiency of TC by TNTs was 82.4%, while it was only 5.9% with original TiO_2 particles. Therefore, TNTs showed much better adsorption ability toward TC than the original TiO_2 particles.

The pH_0 of the solution is recognized as an important factor that significantly affects the removal of TC from aqueous solution. For this reason, the effect of pH_0 value on TC removal was investigated (Fig. 4(a)). It was particularly noteworthy that the process showed an extraordinarily fast initial rate of adsorption, which can be verified by the fact that the amount of adsorbed TC onto TNTs within 3 h almost achieved 90% of that at equilibrium. The rapid initial removal rate of TC could be attributed to the concentration gradient between TC concentration in solution and that at the TNTs surface created at the beginning of the adsorption process [35]. During the initial stage, a large number of vacant surface sites were available for adsorption. With passage of time, the remaining vacant sites were difficult to be occupied because of the repulsive forces between the TC molecules on the TNTs surface and in the bulk solution. Therefore, the removal efficiency became stable after 3 h. As shown in Fig. 4(a), the removal efficiency increased from 70.4 to 82.4% when pH_0 increased from 3 to 5. However, further increasing pH to 7 and 9 led to a decrease in TC removal. The TC removal efficiency was similar at the alkaline pH. The results implied that TNTs were suitable for removing TC under weak acid condition.

The pH effect can be associated with the surface properties of TNTs and the pH-dependent speciation of TC. The point of zero charge (PZC) of TNTs synthesized at 150°C was pH 5.1 [14]. Therefore, the overall charges on the adsorbent surface were positive at pH

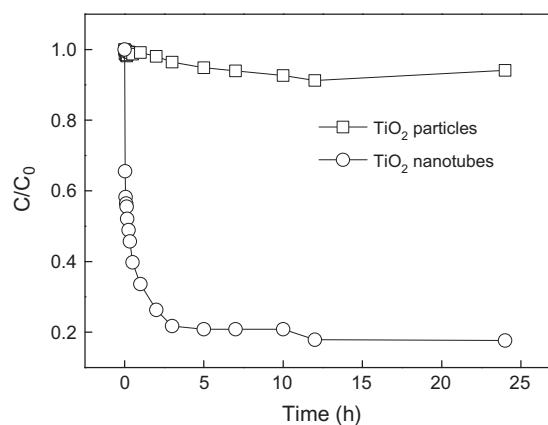


Fig. 3. Removal of TC by TiO_2 particles and TiO_2 nanotubes ($C_0 = 50 \text{ mg/L}$, adsorbent dosage = 0.6 g/L , $\text{pH}_0 = 5$, temperature = 25°C).

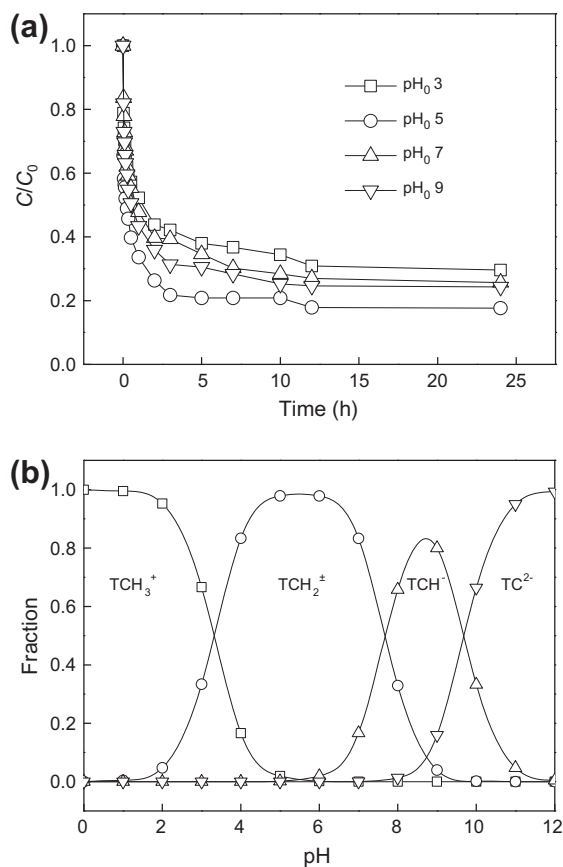


Fig. 4. (a) Effect of initial pH on the removal of TC and (b) speciation of TC under different pH values ($C_0 = 50$ mg/L, adsorbent dosage = 0.6 g/L, temperature = 25 °C).

3 and 5, and were negative at pH 7 and 9. According to Fig. 4(b), TC exists predominantly as (1) a cationic form of TCH_3^+ below pH 3.3, (2) a zwitterion form TCH_2^\pm between pH 3.3 and 7.7, and (3) an anionic form TCH^- or TC^{2-} above pH 7.7. As stated above, in the pH range of 3–9, the removal of TC at pH 5 exhibited a higher removal efficiency. This can be interpreted by the electrostatic repulsion between TNTs and the TC molecule. Increasing pH from 3 to 5, the electrostatic repulsive force between the positively charged TNTs and the cationic forms of TC decreased, and therefore, the removal efficiency increased accordingly. At pH 7 and 9, a negatively charged surface of TNTs was formed and TC existed mainly in its zwitterion and anionic form. The electrostatic repulsion between TNTs and TC retarded the removal of TC compared with that at pH 5.

3.3. Effect of adsorbent dosage on TC removal

The removal efficiency of TC influenced by TNTs dosage is depicted in Fig. 5. It can be seen that the

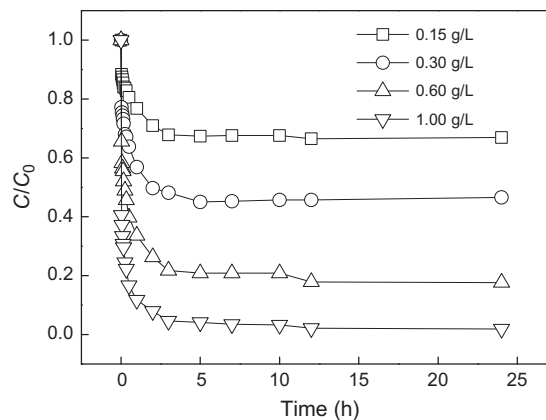


Fig. 5. Effect of adsorbent dosage on the removal of TC ($C_0 = 50$ mg/L, pH₀ 5, temperature = 25 °C).

removal efficiency increased from 33.1 to 98.1% as the TNTs dosage increased from 0.15 to 1.00 g/L. The results might be related to adsorption surface area and available adsorption sites. The increase of adsorbent dosage resulted in the increase of adsorption surface areas and active sites on TNTs. Therefore, the removal efficiency of TC increased accordingly [21]. On the other hand, the amount of TC adsorbed per unit mass of sorbent decreased with an increase in adsorbent amount. When the dosage of TNTs increased from 0.15 to 1.00 g/L, the sorption of TC decreased from 110.24 to 49.05 mg/g. At low adsorbent dosage, the adsorption sites were saturated through the uptake of TC, resulting in saturated TC adsorption. However, the adsorption sites would be excessive for adsorption at higher sorbent dosage, which led to the unsaturation of adsorption sites. In addition, high amount of TNTs might cause aggregation of adsorbents, reducing the surface areas of the adsorbents [21]. Therefore, the amount adsorbed per unit mass of adsorbent decreased.

3.4. Effect of initial TC concentration on TC removal

The efficiency of TC removal affected by different initial TC concentration was investigated. As shown in Fig. 6, with increasing initial concentration from 50 to 125 mg/L, the removal efficiency decreased from 80.7 to 48.9%. When the amount of TNTs remained constant, the number of sorption sites was also constant. By increasing TC concentration, the percent removal would decrease due to the limitation of the sorption sites. On the other hand, as the concentration of TC increased from 50 to 125 mg/L, the sorption increased from 67.22 to 101.98 mg/g. This suggested that by

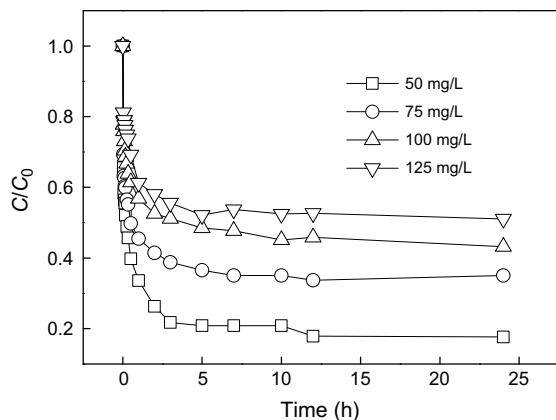


Fig. 6. Effect of initial TC concentration on the removal of TC (pH₀ 5, adsorbent dosage = 0.6 g/L, temperature = 25°C).

increasing the concentration of TC to 2.5 fold, the amount of sorption was increased to about 1.5 fold.

3.5. Adsorption kinetics

In an attempt to examine the adsorption kinetics of TC onto TNTs, the pseudo-first-order and the pseudo-second-order kinetic model were used to fit the experimental data. The pseudo-first-order equation can be expressed by the following linear form:

$$\ln(q_e - q_t) = \ln q_e - k_1 t \quad (2)$$

where q_e and q_t (mg/g) are the amounts of adsorbed TC at equilibrium and at time t , respectively, k_1 (1/min) is the pseudo-first-order rate constant, and t (min) is the contact time. k_1 was calculated from the slope of the plot of $\ln(q_e - q_t)$ vs. t . Another kinetic model is the pseudo-second-order model, which is expressed by:

$$\frac{t}{q_t} = \frac{1}{k_2 q_e^2} + \frac{t}{q_e} \quad (3)$$

where k_2 (g/(mg min)) is the pseudo-second-order rate constant. k_2 could be determined from the intercept of the plot of t/q_t vs. t [36].

The corresponding parameters were determined as listed in Table 1. The pseudo-first-order model showed poor fitting to the experimental data with rather low correlation coefficients (R^2), and the calculated equilibrium adsorption capacities ($q_{e1,cal}$) deviated too much from the measured values ($q_{e,mea}$). This suggested that the pseudo-first-order model failed to describe the adsorption process correctly.

In contrast, linear plots of t/q_t vs. t with correlation coefficients (R^2) higher than 0.99 indicated that the data exhibited a good compliance with the pseudo-second-order kinetic equation (Fig. 7). It was also obvious that $q_{e2,cal}$ calculated by the pseudo-second-order kinetic equation could obtain good agreement with $q_{e,mea}$. The fact that the pseudo-second-order kinetic model provided the best correlation for the system suggested that the mechanism of TC adsorption by TNTs could be described by chemical sorption by covalent forces or ion exchange, which involved valency forces through sharing or exchange of electrons between adsorbent and adsorbate [36].

However, the pseudo-first-order and the pseudo-second-order kinetic models cannot identify the diffusion mechanism during the adsorption process. The experimental data were further fitted with the intraparticle diffusion model, which can be expressed by the following equation:

$$q_t = k_p t^{1/2} + C \quad (4)$$

Table 1
Kinetic parameters for the adsorption of TC by TNTs at 25°C

Kinetic models	Parameters	Initial TC concentration (mg/L)			
		50	75	100	125
Pseudo-first-order kinetic model	$q_{e1,cal}^a$ (mg/g)	34.38	35.31	44.44	61.23
	k_1 (1/min)	0.0184	0.0079	0.0047	0.0112
	R^2	0.8845	0.9087	0.8798	0.9633
Pseudo-second-order kinetic model	$q_{e2,cal}^a$ (mg/g)	67.11	81.97	94.34	102.04
	k_2 (g/(mg min))	0.0016	0.0019	0.0007	0.0008
	R^2	0.9997	0.9998	0.9991	0.9996
	$q_{e,mea}^b$ (mg/g)	64.62	82.87	94.67	101.98

^aThe calculated adsorption capacity at equilibrium, namely q_e in Eqs. (2) and (3), respectively.

^bThe measured adsorption capacity at equilibrium.

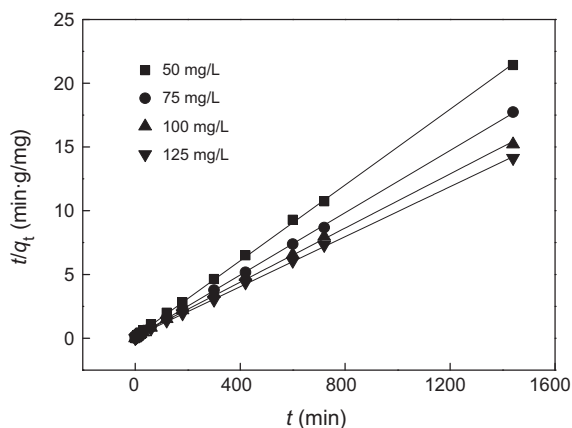


Fig. 7. Pseudo-second-order kinetic model for removal of TC.

where q_t (mg/g) is the amount of TC adsorbed at time t (min), k_p (mg/g min^{1/2}) is the intraparticle diffusion constant, and C is the intercept [37].

When TC solution was mixed with the adsorbent, transport of the TC molecules from the solution through the interface between the solution and adsorbent occurred into the pores of the particles [38]. The plot of q_t vs. $t^{1/2}$ in Fig. 8 showed a double straight-line nature. At the beginning, it was postulated that TC was transported to the external surface of TNTs through film diffusion within a very short time. The first linear part could be due to the entry of TC molecules into the TNTs particle by intraparticle diffusion. The second linear part represented the final equilibrium stage [37]. The values of k_p for the first stage increased from 61.9 to 91.1 mg/g min^{1/2} when the initial TC concentrations increased from 50 to 125 mg/L.

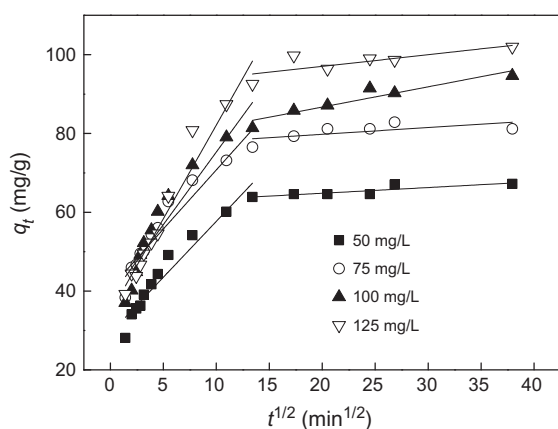


Fig. 8. Intraparticle diffusion kinetics for adsorption of TC onto TNTs.

3.6. Adsorption isotherms

The adsorption isotherm provides much information, such as the distribution of the adsorbate between the adsorbent and liquid phase, and the adsorption capacity of the adsorbent, which is essential in the design of the adsorption system. Hence, the equilibrium data were subject to simulate with three isotherm models, i.e. Langmuir, Freundlich, and Temkin isotherm models.

The Langmuir model assumes that monolayer surface adsorption occurs on specific homogeneous sites and no interaction exists between the adsorbed pollutants. The equation for this model can be written as follows:

$$\frac{C_e}{q_e} = \frac{1}{q_{max}K_L} + \frac{C_e}{q_{max}} \quad (5)$$

where C_e (mg/L) is the equilibrium solute (TC) concentration, q_e (mg/g) is the amount of TC adsorbed at equilibrium, q_m (mg/g) is the maximum adsorption capacity, and K_L (L/mg) is the Langmuir constant related to the free energy of adsorption. Plotting C_e/q_e vs. C_e will give a straight line with slope $1/q_{max}$ and intercept $1/(q_{max} \cdot K_L)$ if the Langmuir model is held.

Based on the essential characteristic of the Langmuir model, an adsorption system can be evaluated as “favorable” or “unfavorable” in terms of a dimensionless constant, the separation factor R_L , as defined by:

$$R_L = \frac{1}{1 + bC_0} \quad (6)$$

where C_0 (mg/L) is the initial concentration of TC and b (L/mg) is the Langmuir constant. According to the values of R_L , the adsorption process may be classified as irreversible ($R_L = 0$), favorable ($0 < R_L < 1$), linear ($R_L = 1$), and unfavorable ($R_L > 1$).

The Freundlich isotherm is an empirical equation describing heterogeneous surface adsorption. The linear form of the equation is usually expressed as follows:

$$\ln q_e = \ln K_F + \frac{1}{n} \ln C_e \quad (7)$$

where K_F (mg/g) is the Freundlich constant related to the adsorption capacity of the adsorbent, and $1/n$ represents the heterogeneity of the adsorption surface and is related to the magnitude of the adsorption driving force. Both constants are obtained from the slope and intercept of the linear plot of $\ln q_e$ vs. $\ln C_e$.

Table 2

Langmuir, Freundlich, and Temkin isotherm constants for the adsorption of TC onto TNTs

Langmuir			Freundlich			Temkin		
q_m (mg/g)	K_L (L/mg)	R^2	K_F (mg/g)	n	R^2	A (L/g)	B (J/mol)	R^2
113.6	0.1196	0.9947	39.99	4.450	0.9898	3.571	133.19	0.9794

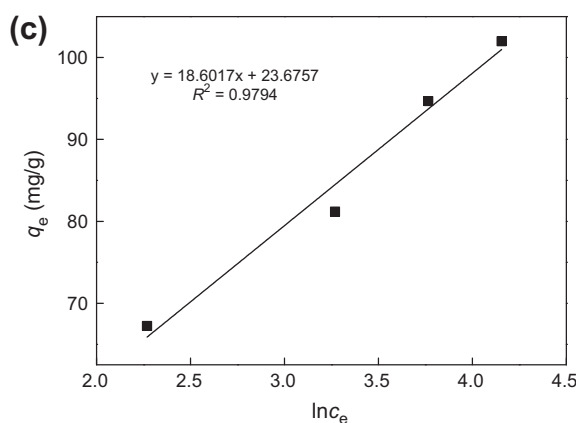
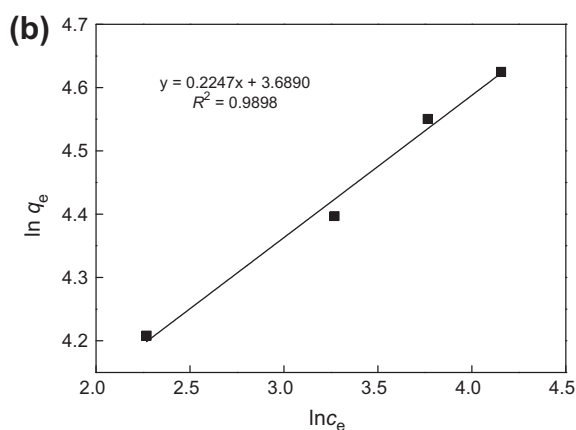
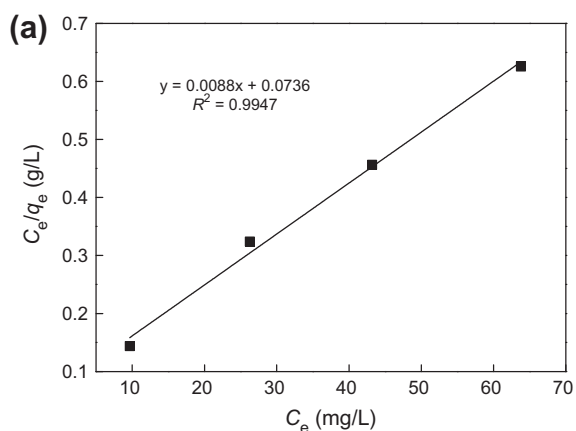


Fig. 9. Adsorption isotherms of TC: (a) Langmuir, (b) Freundlich, and (c) Temkin models (pH₀ 5, adsorbent dosage = 0.6 g/L, temperature = 25 °C, contact time = 24 h).

The Temkin model is different from the above-mentioned isotherm models because it considers the effect of the interaction between the adsorbent and adsorbate. This isotherm model is represented as follows:

$$q_e = \frac{RT}{B} \ln A + \frac{RT}{B} \ln C_e \quad (8)$$

where A (L/g) and B (J/mol) are the Temkin constants, R (J/(mol K)) is the ideal gas constant, and T is the absolute temperature. A plot of q_e vs. $\ln C_e$ is used to calculate the values of A and B .

Table 2 lists the constants and correlation coefficients involved in the three isotherm models. It was apparent that the experimental data fitted much better with the Langmuir isotherm than the other two isotherms, as correlation coefficient R^2 for the Langmuir isotherm (0.9947) was the highest (Fig. 9). The fact that the adsorption isotherms of TC exhibited good Langmuir behaviors implied the existence of homogeneous active sites within the TNTs and the monolayer adsorption of TC on the adsorbent. Also, the corresponding monolayer saturated adsorption capacity was 113.6 mg/g at 25 °C according to the fitting result. Moreover, in our experiments the values of R_L at different initial concentration of TC were between 0 and 1, suggesting that the adsorption of TC on the surface of TNTs was favorable. The results indicated that TNTs could be employed as promising adsorbents for TC removal.

4. Conclusions

TNTs were prepared through an alkaline hydrothermal treatment of TiO₂ particles with 10 M NaOH aqueous solution. The possible application for the removal of TC was investigated. The analyses of N₂ adsorption/desorption isotherms showed that the TNTs exhibited larger specific surface areas of 155.78 m²/g and higher pore volumes of 0.38 cm³/g. Furthermore, the results of XRD revealed that the main component of TNTs was H₂Ti₃O₇. Batch adsorption tests demonstrated that the removal of TC was affected by various conditions such as initial solution

pH, adsorbent dosage, and initial TC concentration. The maximum removal efficiency of TC was detected at initial pH 5. The removal efficiency increased with the increase of TNTs dosage and the decrease of initial TC concentration. The kinetic study indicated that the removal of TC onto TNTs followed the pseudo-second-order kinetic model. The study on equilibrium adsorption revealed that the Langmuir model was the most appropriate model to describe TC adsorption behaviors. The monolayer maximum adsorption capacities of TC were found to be 113.6 mg/g. Consequently, the TNTs could be a potential adsorbent to efficiently remove TC due to the high adsorption capacity.

Acknowledgments

This study was supported by Natural Science Foundation of China (Grant Nos. 20977069 and 21211130108) and Natural Science Foundation of Hubei Province, China (Grant No. 2012FFA089).

References

- [1] S. Jain, R.K. Vyas, P. Pandit, A.K. Dalai, Adsorption of antiviral drug, acyclovir from aqueous solution on powdered activated charcoal: Kinetics, equilibrium, and thermodynamic studies, *Desalin. Water Treat.* 52 (2014) 4953–4968.
- [2] M. Maheshwari, R.K. Vyas, M. Sharma, Kinetics, equilibrium and thermodynamics of ciprofloxacin hydrochloride removal by adsorption on coal fly ash and activated alumina, *Desalin. Water Treat.* 51 (2013) 7241–7254.
- [3] N. Oturan, J. Wu, H. Zhang, V.K. Sharma, M.A. Oturan, Electrocatalytic destruction of the antibiotic tetracycline in aqueous medium by electrochemical advanced oxidation processes: Effect of electrode materials, *Appl. Catal. B: Environ.* 140–141 (2013) 92–97.
- [4] J. Wu, H. Zhang, N. Oturan, Y. Wang, L. Chen, M.A. Oturan, Application of response surface methodology to the removal of the antibiotic tetracycline by electrochemical process using carbon-felt cathode and DSA (Ti/RuO₂-IrO₂) anode, *Chemosphere* 87 (2012) 614–620.
- [5] H. Zhang, F. Liu, X. Wu, J. Zhang, D. Zhang, Degradation of tetracycline in aqueous medium by electrochemical method, *Asia-Pac. J. Chem. Eng.* 4 (2009) 568–573.
- [6] Z. Zhang, H. Lan, H. Liu, J. Qu, Removal of tetracycline antibiotics from aqueous solution by amino-Fe (III) functionalized SBA15, *Colloids Surf., A: Physicochem. Eng. Aspects* 471 (2015) 133–138.
- [7] Y. Gao, Y. Li, L. Zhang, H. Huang, J. Hu, S.M. Shah, X. Su, Adsorption and removal of tetracycline antibiotics from aqueous solution by graphene oxide, *J. Colloid Interface Sci.* 368 (2012) 540–546.
- [8] M. Klavarioti, D. Mantzavinos, D. Kassinos, Removal of residual pharmaceuticals from aqueous systems by advanced oxidation processes, *Environ. Int.* 35 (2009) 402–417.
- [9] Y. Wang, H. Zhang, J.H. Zhang, L. Chen, Q.Q. Huang, J. Wu, F. Liu, Degradation of tetracycline in aqueous media by ozonation in an internal loop-lift reactor, *J. Hazard. Mater.* 192 (2011) 35–43.
- [10] L. Hou, H. Zhang, X. Xue, Ultrasound enhanced heterogeneous activation of peroxydisulfate by magnetite catalyst for the degradation of tetracycline in water, *Sep. Purif. Technol.* 84 (2012) 147–152.
- [11] Y. Wang, H. Zhang, L. Chen, Ultrasound enhanced catalytic ozonation of tetracycline in a rectangular air-lift reactor, *Catal. Today* 175 (2011) 283–292.
- [12] X. Bao, Z. Qiang, W. Ling, J.H. Chang, Sonochemical synthesis of MFe₂O₄ magnetic nanoparticles for adsorptive removal of tetracyclines from water, *Sep. Purif. Technol.* 117 (2013) 104–110.
- [13] L. Hou, H. Zhang, L. Wang, L. Chen, Ultrasound-enhanced magnetite catalytic ozonation of tetracycline in water, *Chem. Eng. J.* 229 (2013) 577–584.
- [14] H.Y. Niu, J.M. Wang, Y.L. Shi, Y.Q. Cai, F.S. Wei, Adsorption behavior of arsenic onto protonated titanate nanotubes prepared via hydrothermal method, *Microporous Mesoporous Mater.* 122 (2009) 28–35.
- [15] L. Zhang, X. Song, X. Liu, L. Yang, F. Pan, J. Lv, Studies on the removal of tetracycline by multi-walled carbon nanotubes, *Chem. Eng. J.* 178 (2011) 26–33.
- [16] P.H. Chang, J.S. Jean, W.T. Jiang, Z. Li, Mechanism of tetracycline sorption on rectorite, *Colloids Surf., A: Physicochem. Eng. Aspects* 339 (2009) 94–99.
- [17] L. Huang, C. Shi, B. Zhang, S. Niu, B. Gao, Characterization of activated carbon fiber by microwave heating and the adsorption of tetracycline antibiotics, *Sep. Sci. Technol.* 48 (2013) 1356–1363.
- [18] L. Huang, M. Wang, C. Shi, J. Huang, B. Zhang, Adsorption of tetracycline and ciprofloxacin on activated carbon prepared from lignin with H₃PO₄ activation, *Desalin. Water Treat.* 52 (2014) 2678–2687.
- [19] M. Eugenia Parolo, M.J. Avena, M.C. Savini, M.T. Baschini, V. Nicotra, Adsorption and circular dichroism of tetracycline on sodium and calcium-montmorillonites, *Colloids Surf., A Physicochem. Eng. Aspects* 417 (2013) 57–64.
- [20] H. Li, X. Zhong, H. Zhang, L. Xiang, S. Royer, S. Valange, J. Barrault, Ultrasound-assisted removal of tetracycline from aqueous solution by mesoporous alumina, *Water Sci. Technol.* 69 (2014) 819–824.
- [21] L. Xiong, C. Chen, Q. Chen, J. Ni, Adsorption of Pb(II) and Cd(II) from aqueous solutions using titanate nanotubes prepared via hydrothermal method, *J. Hazard. Mater.* 189 (2011) 741–748.
- [22] E. Morgado Jr., M.A.S. de Abreu, O.R.C. Pravia, B.A. Marinkovic, P.M. Jardim, F.C. Rizzo, A.S. Araújo, A study on the structure and thermal stability of titanate nanotubes as a function of sodium content, *Solid State Sci.* 8 (2006) 888–900.
- [23] T. Kasuga, M. Hiramatsu, A. Hoson, T. Sekino, K. Niihara, Formation of titanium oxide nanotube, *Langmuir* 14 (1998) 3160–3163.
- [24] C.K. Lee, S.S. Liu, L.C. Jiang, C.C. Wang, M.D. Lyu, S.H. Hung, Application of titanate nanotubes for dyes

- adsorptive removal from aqueous solution, *J. Hazard. Mater.* 148 (2007) 756–760.
- [25] C.K. Lee, K.S. Lin, C.F. Wu, M.D. Lyu, C.C. Lo, Effects of synthesis temperature on the microstructures and basic dyes adsorption of titanate nanotubes, *J. Hazard. Mater.* 150 (2008) 494–503.
- [26] C.K. Lee, C.C. Wang, L.C. Juang, M.D. Lyu, S.H. Hung, S.S. Liu, Effects of sodium content on the microstructures and basic dye cation exchange of titanate nanotubes, *Colloids Surf., A: Physicochem. Eng. Aspects* 317 (2008) 164–173.
- [27] L. Xiong, Y. Yang, J. Mai, W. Sun, C. Zhang, D. Wei, Q. Chen, J. Ni, Adsorption behavior of methylene blue onto titanate nanotubes, *Chem. Eng. J.* 156 (2010) 313–320.
- [28] W. Liu, T. Wang, A.G.L. Borthwick, Y. Wang, X. Yin, X. Li, J. Ni, Adsorption of Pb^{2+} , Cd^{2+} , Cu^{2+} and Cr^{3+} onto titanate nanotubes: Competition and effect of inorganic ions, *Sci. Total Environ.* 456–457 (2013) 171–180.
- [29] G. Sheng, L. Ye, Y. Li, H. Dong, H. Li, X. Gao, Y. Huang, EXAFS study of the interfacial interaction of nickel(II) on titanate nanotubes: Role of contact time, pH and humic substances, *Chem. Eng. J.* 248 (2014) 71–78.
- [30] G. Sheng, H. Dong, R. Shen, Y. Li, Microscopic insights into the temperature-dependent adsorption of Eu(III) onto titanate nanotubes studied by FTIR, XPS, XAFS and batch technique, *Chem. Eng. J.* 217 (2013) 486–494.
- [31] G. Sheng, B. Hu, Role of solution chemistry on the trapping of radionuclide Th(IV) using titanate nanotubes as an efficient adsorbent, *J. Radioanal. Nucl. Chem.* 298 (2013) 455–464.
- [32] S. Sreekantan, L.C. Wei, Study on the formation and photocatalytic activity of titanate nanotubes synthesized via hydrothermal method, *J. Alloys Compd.* 490 (2010) 436–442.
- [33] Q. Chen, W. Zhou, G. Du, L.M. Peng, Trititanate nanotubes made via a single alkali treatment, *Adv. Mater.* 14 (2002) 1208–1211.
- [34] G.S. Guo, C.N. He, Z.H. Wang, F.B. Gu, D.M. Han, Synthesis of titania and titanate nanomaterials and their application in environmental analytical chemistry, *Talanta* 72 (2007) 1687–1692.
- [35] M. Kaur, M. Datta, Adsorption equilibrium and kinetics of toxic dye-erythrosine B adsorption onto montmorillonite, *Sep. Sci. Technol.* 48 (2013) 1370–1381.
- [36] Y.S. Ho, G. McKay, Pseudo-second order model for sorption processes, *Process Biochem.* 34 (1999) 451–465.
- [37] P. Luo, Y. Zhao, B. Zhang, J. Liu, Y. Yang, J. Liu, Study on the adsorption of Neutral Red from aqueous solution onto halloysite nanotubes, *Water Res.* 44 (2010) 1489–1497.
- [38] N.S. Awwad, H.M.H. Gad, M.I. Ahmad, H.F. Aly, Sorption of lanthanum and erbium from aqueous solution by activated carbon prepared from rice husk, *Colloids Surf., B: Biointerfaces* 81 (2010) 593–599.